LBL--19114

DE85 009941

Pion Production and the Nuclear Equation of State

J.W. Harris, G. Odyniec, H.G. Pugh, L.S. Schroeder and M.L. Tincknell
Lawrence Berkeley Laboratory, University of California 9513034
Berkeley, California 94720 U.S.A.

R. Bock, R. Brockmann, A. Sandoval, R. Stock and H. Ströbele
Gesellschaft für Schwerionenforschung
D-6100 Darmstadt, West Germany 9200078

R.E. Renfordt and D. Schall
Institut für Hochenergiephysik, Universität Heidelberg 2972000
Heidelberg, West Germany

D. Bangert and W. Rauch
Fachbereich Physik, Universität Marburg 9200058
D-3550 Marburg, West Germany

A. Dacal, K. Guerra and M.E. Ortiz
Instituto de Física, Universidade Nacional Autónoma de Mexico 6505050
Mexico City, 21 D.F., Mexico

and

K.L. Wolf
Cyclotron Laboratory, Texas A & M University 618 3000
College Station, Texas 77843.

Introduction

There has been considerable recent interest in the nuclear equation of state and how it may be determined in relativistic nucleus-nucleus collisions. In these collisions extremely high temperatures are reached and compression to densities several times that of normal nuclear matter are predicted. This affords us the unique opportunity to study, in a somewhat controlled manner, the behavior of nuclear matter under these extreme conditions. If the observables that are measured in experiments can be related in a quantitative way to state variables of the system then the equation of state can be extracted. This relation plays a very important role in understanding the formation and collapse of supernovae [1] and the stability and structure of neutron stars [2]. Furthermore, it can be used to test and constrain field theoretical approaches [3,4] to nuclear matter and to help to better understand the dynamics of high energy nucleus-nucleus collisions.

In this presentation the relationship between the nuclear equation of state and relativistic nucleus-nucleus collisions will be discussed with an emphasis on how to extract the former. That a high density state of the collision should exist will be shown. One observable, namely the pion multiplicity, will be shown to survive the succeeding stages of the collision process to provide information on the equation

of state at high densities. The resulting equation of state will be presented and discussed in the light of recent theoretical developments.

Relativistic Nucleus-Nucleus Collisions and the Nuclear Equation of State

In the collision of two heavy nuclei at velocities approaching the speed of light three distinct stages of the reaction are predicted. On the microscopic level as the two nuclei collide, binary nucleon-nucleon collisions will initially dominate. As the nuclei continue to interpenetrate, successive nucleon-nucleon collisions occur in the overlap region. In macroscopic terms this results in conversion of part of the energy of relative motion into internal energy and an increase in the temperature and density in the overlap region. This first stage of the collision is the compression stage. The dynamics of the collision process can easily be seen in predictions of the intranuclear cascade model [5] shown in Fig.1 for central collisions of 1.0 GeV/n La + La. Plotted logarithmically are the a) baryon density, b) number of baryon-baryon collisions per unit time, and c) number of produced particles (pions + delta resonances) in the system as a function of time in the collision. The number of created particles reflects part of the energy that is transformed from relative motion into other degrees of freedom. All three variables in Fig.1 are observed to increase rapidly during the compression stage. At a somewhat later time, in the middle of the collision process, the baryon density becomes relatively constant for a period of time before rapidly decreasing exponentially. This plateau in density represents the second stage of the collision, namely the high density state. At this time the baryon-baryon collision rate peaks at approximately 90 collisions per fm/c and the number of created particles in this model reaches a maximum. The exponential decrease in density, the rapid decrease in the collision rate, and a saturation of the abundance of produced particles characterizes the third stage - expansion.

The equation describing the energy of a system of particles can be written schematically as

$$E(\rho,T) = E_T(\rho,T) + W(\rho) \ , \tag{1}$$

where $E(\rho,T)$ is the total center-of-mass energy, $E_T(\rho,T)$ the thermal excitation energy, and $W(\rho)$ the energy associated with the potential degrees of freedom. The ρ and T represent the density and temperature of the system, respectively. To obtain the equation of state the pressure of the system is found by taking the partial derivative of the above equation with respect to the density at constant entropy S

$$P(\rho,T) = \rho^2 \left(\frac{\partial E(\rho,T)}{\partial \rho}\right)_{dS=0} \ . \tag{2}$$

This yields

$$P(\rho,T) = \rho^2 \left(\left(\frac{\partial E_T(\rho,T)}{\partial \rho}\right)_{dS=0} + \left(\frac{dW(\rho)}{d(\rho)}\right)\right) \ , \tag{3}$$

where the partial derivative term is the thermal pressure and the second term is the compression. This second term which describes the response of the potential

energy to changes in density is often referred to as the nuclear equation of state, as will be done here. Several of the state variables introduced above and necessary to describe the system can be related to physical observables which are accessible, to some degree, in relativistic nucleus-nucleus collisions. These are listed below:

STATE VARIABLES	OBSERVABLES
$E_T(\rho, T)$	abundance of produced particles (pion multiplicities) (strange particle yields)
$S(\rho, T)$	ratios of various types of particles (deuteron/proton ratios)
$P(\rho, T)$	distributions of particles in phase-space (asymmetric or radial flow)

How can the equation of state $dW(\rho)/d\rho$ be determined? In the following it will be shown that a high density state exists in these collisions facilitating a description in terms of state variables. Furthermore, this state has observables associated with the state variables which should survive the succeeding expansion stage of the collision. Specifically, the pion multiplicity will be used to determine the thermal energy content of the system and along with the total energy in Equ.1 will provide information on $W(\rho)$ to yield the equation of state. The relationship between other possible observables such as flow and the d/p ratios to the equation of state will be discussed in two other presentations [6,7] of this meeting.

Pion Production in Relativistic Nucleus-Nucleus Collisions

The sensitivity of the pion production in relativistic nucleus-nucleus collisions to the nuclear equation of state was initially pointed out by several authors [8,9,10,11]. The first quantitative results on the sensitivity of pion production to the compressibility of nuclear matter were calculated [10] using hydrodynamics and are shown in Fig.2a. A significantly lower number of pions are predicted when a stiff (higher compressional energy at a given baryon density) nuclear equation of state is assumed. Furthermore, in the presence of a density isomer a sharp rise in the number of pions produced as a function of incident energy was predicted as seen in Fig.2b. A subsequent measurement [12] of the negative pion multiplicity $< n_{\pi^-} >$ for central collisions in the Ar + KCl system at incident energies of 360 to 1800 MeV/n is shown in Fig.3. The energy-dependence of the $< n_{\pi^-} >$ is linear with no sharp deviations which might suggest the presence of density isomers. Recent results [13] at an incident laboratory energy of 3.6 GeV/n for Ne + Ne show a continuation of this linear dependence to higher energies. Of more general importance is the determination of what can be learned from these measurements about the nuclear equation of state. In order to be able to extract a functional relationship between state variables of the system, like pressure and density, a better understanding of the dynamic behavior of the collision is necessary. In particular, the degree to

which thermal and chemical equilibrium are reached and maintained during a high energy nucleus-nucleus collision will determine whether the pion multiplicity can in fact be used to extract information on the nuclear equation of state.

Thermal and Chemical Equilibrium

The extent to which thermal and chemical equilibrium is reached in relativistic nucleus-nucleus collisions has been estimated by several authors [14,15,16,17] using statistical thermodynamics. Thermal equilibrium may be viewed simply as an equipartition of the available energy into the various degrees of freedom. Chemical equilibrium occurs when the reaction rates for formation and breakup of a constituent are equal, thereby establishing the abundances of the various species in the system. At Bevalac energies ($E_{lab} \sim 2\ GeV/n$) the system can be considered to be a gas of nucleons, delta-particles, and pions. The rates governing the approach to equilibrium are determined by successive collisions on the microscopic level between these constituent particles. The rate equations [15,16,17] can be solved to yield the chemical equilibration time constant

$$\tau_{equ} = \frac{2\rho_\Delta^{equ}}{\rho_N^2 < \sigma_{NN \rightarrow N\Delta} v >} \ , \tag{4}$$

where ρ_Δ^{equ} and ρ_N are the delta and nucleon densities in equilibrium. The time constant for chemical equilibrium is governed by the inelastic reaction $NN \leftrightarrow N\Delta$ rate. The $< \sigma_{NN \leftrightarrow N\Delta} v >$ is the thermal energy average of the cross section for $NN \leftrightarrow N\Delta$ times the relative velocity v of the particle pair. The thermal equilibration time constant can be calculated in a similar way by using the total cross section rather than the inelastic one. This will inherently yield a shorter equilibration time for thermal equilibrium than for chemical equilibrium since $\sigma_{tot} > \sigma_{NN \leftrightarrow N\Delta}$. If τ_{equ} is less than the lifetime of a given state of the system $\Delta\tau_{state}$, then equilibrium is possible.

As a first estimate of the extent of chemical equilibrium in the high density stage a collision of an equal mass system at 1 GeV/n is considered. Representative values [15,16,17] are temperature $T = 100$ MeV, $\rho_\Delta^{equ} = 0.2\rho_N \cong 0.6\rho_0$ with $\rho_N = 3\rho_0$ and ρ_0 the normal nuclear density, and $< \sigma_{NN \leftrightarrow N\Delta} v > \cong 1.5 \times 10^{23} fm^3 s^{-1}$. The chemical equilibration time constant is found to be

$$\tau_{chemical} \approx 6 \times 10^{-24} s \ , \tag{5}$$

and the thermal time constant

$$\tau_{thermal} \approx 3 \times 10^{-24} s \ . \tag{6}$$

These should be compared to the lifetime of the high density stage which from the cascade calculation is

$$\Delta\tau_\rho(Ar + KCl) \approx 4fm/c = 1.3 \times 10^{-23} s \ , \tag{7}$$

for $Ar + KCl$ and

$$\Delta\tau_\rho(La + La) \approx 8fm/c = 2.6 \times 10^{-23}s \ , \tag{8}$$

for $La + La$. Since the time scales to reach equilibrium in both systems are smaller than the lifetime of the high density stage, namely

$$\tau_{thermal} < \tau_{chemical} < \Delta\tau_\rho \ , \tag{9}$$

both thermal and chemical equilibrium should exist for medium to heavy mass systems at the end of the high density stage.

Once equilibrium among the nucleons, deltas and pions is established in the high density stage the system can be described in terms of statistical thermodynamics using state variables and observables. However, effects of the expansion phase upon these variables and observables must be considered to be able to determine which survive to provide viable information on the system at high density. The expansion can, in principle, proceed along any path between isoergic (constant energy) and isentropic (constant entropy). Isoergic expansion, which is assumed in most thermal models - most notably the fireball model [18] - is accompanied by a slow decrease in the temperature of the system and an increase in the number of produced particles, in this case pions and deltas. During isentropic expansion the system will shrink in momentum space to counteract its growth in position space. This can be considered as radial flow, where the temperature drops rapidly as randomly-directed kinetic energy is converted into radial collective motion, accompanied by a decrease in the pion and delta abundances. Isentropic expansion is assumed in the hydrodynamic models and has been observed [19] in the cascade calculations. The central density in the cascade calculations decreases exponentially during expansion with a characteristic time of 10^{-23} s as shown in Fig.1. An estimate of the equilibration times for the two extreme cases of expansion can be made. Assuming that the expansion proceeds along a path somewhere between isoergic and isentropic, the chemical equilibration time constant from Equ.4 at $\rho = 0.7\rho_0$ is

$$3 \times 10^{-23}s < \tau_{chemical} < 2 \times 10^{-22}s \ , \tag{10}$$

both limits being much longer than the characteristic time of expansion $10^{-23}s$. ***Chemical equilibrium among nucleons, deltas, and pions cannot be maintained to late times in the expansion process*** [20]. The pion degree of freedom, which is the total number of pions and deltas in the system, will freeze-out at an earlier time closer to the end of the high density stage. This is contrary to the assumptions made in the fireball [18] and hydrodynamic [21] model calculations where the freeze-out densities were assumed to be between $\rho = (0.5 \rightarrow 1.0)\rho_0$.

The thermal equilibration time constant can be determined in a similar manner using Equ.4 where the large $\sigma_{\pi N \leftrightarrow \Delta}$ will dominate the reaction processes. The time constants for the limiting cases at $\rho = 0.7\rho_0$ are

$$2 \times 10^{-24}s < \tau_{thermal} < 1 \times 10^{-23}s \ , \tag{11}$$

where the shortest time is for isoergic expansion and the longer one for isentropic expansion. Therefore, ***thermal equilibrium of the nucleons, deltas, and pions should continue on into the expansion phase.*** For reasonable assumptions about the expansion mechanism the equilibration times can be summarized by

$$\tau_{thermal} \leq \Delta\tau_{expansion} < \tau_{chemical} \ . \tag{12}$$

The pion spectra (temperatures)[22] and source sizes taken from pion-interferometry measurements [23] will reflect the thermal freeze-out in the later stages of expansion, while the total pion multiplicity after decay of the remaining deltas is established by chemical freeze-out near the end of the high density stage.

In light of identifying other prospective observables of the high density stage it is informative to estimate the equilibration times associated with nuclear cluster formation and strange particle production. Being produced-particles like pions and deltas, the strange particles may reflect the early stage or the high density stage of the collision. The nuclear clusters would not be expected to form until late in the reaction when nuclear densities have fallen below ρ_0 and clusters could finally coexist among nucleons. However, in this case they still could reflect the entropy [24] of the system if chemical equilibrium were to exist among the nuclear particle species. The ratios of various nuclear clusters would then determine the entropy in the late stages of the reaction and the high density stage as well if the expansion were indeed isentropic. Taking values from Ref.[16], it is found that

$$\tau_{cluster} \approx 1 \times 10^{-23} s \approx \Delta\tau \left(\frac{2}{3} \rightarrow \frac{1}{3}\right) \rho_0 \ . \tag{13}$$

These values suggest that cluster equilibrium is possible but somewhat questionable, particularly for light nucleus-nucleus systems, noncentral collisions, and high incident energies. In all three of these cases the estimated equilibration time would be an underestimate.

The cross sections that govern strange particle production at Bevalac energies are small, approximately 15 μbarns. This results in very long equilibration times [17] for strange particle production

$$\tau_{strange} \geq 10^{-22} s \gg \Delta\tau_{\rho} \ or \ \Delta\tau_{expansion} \ . \tag{14}$$

Thus, one would not expect chemical or thermal equilibrium for the strange particles. In fact, since the cross sections are so small the additional energy provided by the Fermi motion would favor production primarily in the compression stage where binary nucleon-nucleon collisions dominate.

Pion Multiplicity as a Probe of the Nuclear Equation of State

The pion multiplicity can now be used to determine the thermal energy content of the system in the high density stage assuming the ideal case of chemical and thermal equilibrium where chemical freeze-out occurs at the end of the high density

stage [20]. The total excitation energy per baryon in the center of mass for a system at temperature T and density ρ can be written as

$$E - m_N = E_B(T) + < n_\pi > E_\pi + < n_\Delta >< m^* > + W(\rho, T = 0) + E_{flow} \ , \quad (15)$$

where the left-hand side is the beam c.m. kinetic energy per nucleon. The first three terms on the right are the thermal energy contained in baryons, pions and resonance mass excess m^*. The fourth term is the nuclear matter energy at $T = 0$ and density ρ while the last term is the flow kinetic energy at ρ. All terms on the right side are taken per baryon. The nuclear matter energy can now be extracted assuming that the pion multiplicity is established at the time of maximum compression in the high density stage when the flow kinetic energy is zero. The flow kinetic energy should appear later as the potential energy is reconverted to kinetic energy in the expansion [21,25]. Therefore, at the time of maximum density Equ.15 becomes

$$\epsilon = E_T(\rho, n_\pi + n_\Delta) + E_c(\rho, T = 0) \ , \quad (16)$$

and

$$E_c = W(\rho, T = 0) - W_0 \ , \quad (17)$$

where ϵ is the incident kinetic energy in the c.m., E_T the thermal energy, E_c the compressional energy, and W_0 the binding energy of ground state nuclear matter. Each term in Equ.16 is determined per participant baryon. The Fermi degeneracy energy contribution to $W(\rho, T = 0)$ will be ignored in order to extract the equation of state from Equ.16 in a direct and simple manner. The compressional energy E_c will only contain potential energy contributions with all the kinetic energy resident in the thermal energy E_T term. The equation of state will be determined, within the limitations of the present model, by considering the thermal energy as the only source of pion and resonance production. By so doing the compressional energy can be extracted knowing the incident energy in the c.m. The limitations of this approach have recently been examined by Sano [26].

The compressional energy will be determined by a comparision of the observed pion multiplicity with models which only contain thermal energy and ignore the nonthermal component E_c. In a previous approach [27] the intranuclear cascade model was used and in this presentation a relativistic chemical model [11,28] containing fermions and bosons will be used to calculate the thermal energy contribution. The presence of compression in the collision simply offsets the thermal energy scale with respect to the beam energy ϵ as seen in Equ.16. The total pion multiplicity determined from experiment at an energy ϵ will determine E_T and therefore $E_c(\epsilon)$. The compressional energy $E_c(\epsilon)$ can be plotted as a function of baryon density ρ once $\rho(\epsilon)$ is known. The cascade dependence of $\rho(\epsilon)$ is plotted in Fig.4. For the chemical model the baryon density is calculated assuming shock compression by using the relativistic Rankine-Hugoniot relation [8]

$$\frac{\rho}{\rho_0} = \frac{\gamma_{c.m.}}{(1 - \rho_0 E_{lab}/2P)} \ . \quad (18)$$

The ρ/ρ_0 is the baryon density associated with the shock compression of a medium at rest in the center of mass where $\gamma_{c.m.}$ is the beam Lorentz factor with respect

to the c.m. frame for incident laboratory kinetic energy per nucleon E_{lab}. The P is the pressure of the medium which can be related to the temperature T and $W(\rho, T = 0)$ by

$$P = \rho^2 \frac{dW(\rho)}{d\rho} + \rho T \ . \tag{19}$$

In this approximation the usual sum over the partial pressures of the constituent N,Δ and π gases is replaced by the term ρT. This corresponds to a classical approximation to the N, Δ pressure and ignores the pressure due to thermal π's which is a small correction at the high temperatures considered [11,29]. Equations 16-19 were solved self-consistently using ϵ and ρ/ρ_0 as input into the chemical model [28] and comparing the output $< n_\pi >$ with the experimental $< n_\pi >$ to extract E_T and thus E_c. The temperature used in Equ.19 comes from the chemical model. This procedure of using the chemical model with Rankine-Hugoniot compression is, in essence, a simple hydrodynamic model.

In order to make a reasonable comparison between the experimental pion multiplicities and the chemical model predictions which assume shock compression, collisions at small impact parameters must be selected. This can be accomplished by extrapolating the minimum bias data to zero impact parameter as shown in Fig.5. An event-by-event determination of the negative pion multiplicity was made as a function of the number of protons participating in the reaction for Ar + KCl at incident energies of 0.57 to 1.8 GeV/n using the streamer chamber at the Bevalac. The results for energies from 1.0 to 1.8 GeV/n are presented. Since the $< n_{\pi^-} >$ is observed to rise linearly with the number of protons (and therefore nucleons) participating in the reaction, an extrapolation to the limit where all protons (neutrons) participate is straghtforward. The limiting values of $< n_{\pi^-} >$ corresponding to total disintegration of both incident nuclei represent those for zero impact parameter collisions and occur at the arrow $Q = Z_{Ar} + \overline{Z_{KCl}}$ in Fig.5. The isobar model is then used to obtain the total pion multiplicity per baryon $< n_{\pi^-} >$ from $< n_\pi > \approx 3 < n_{\pi^-} >$. This procedure enables the extraction of the pion multiplicities for truly head-on collisions independent of experimental trigger biases.

The results of the pion multiplicity comparisons as a function of energy are shown in Fig.6. The cascade model predictions, made previously [27], and those of the chemical model are in fairly close agreement. Both clearly overpredict the experimentally observed pion multiplicities. The resulting compressional energies represented by the horizontal arrows are similar in both models. Note, however, that neither the cascade nor the experiment may have reached perfect equilibrium and that corrections due to surface effects may still be necessary.

Pion multiplicities have also been measured for the heavier system $^{139}La + ^{139}La$ at incident energies of 534, 739, 992 and 1166 MeV/n in a central trigger mode corresponding to impact parameters $b \lesssim 0.25 b_{max}$. Extrapolation to zero impact parameter is much more difficult for this heavy system than for the Ar + KCl system. A 384 element forward scintillator array was used in addition to the streamer chamber to distinguish the number of participants in the events. This work is still in progress and a comparison with the chemical model is not yet possible. However, a comparison can be made between the central trigger data and the

cascade model as in Ref.[27] to extract preliminary compressional energies. The trigger cross section and the geometric model are used to determine the impact parameter range of the experiment for use in the cascade. The resulting negative pion multiplicities are shown in Fig.7 for the central trigger data ($b \lesssim 0.25 b_{max}$) and the cascade. Similar data for the Ar + KCl system at $b \lesssim 0.33 b_{max}$ are also presented in Fig.7. The absolute value of the pion multiplicity is noticably larger for the heavier system but the ratio of pions to participants cannot yet be determined as stated above. Following the prescription of Ref.[27] the compressional energy is simply the length of the horizontal arrows. The results of the cascade and chemical model analyses for the Ar + KCl data at zero impact parameter and the preliminary cascade model analysis of the La + La data at ($b \lesssim 0.25 b_{max}$) are presented in Fig.8. The extracted compressional energies as a function of the baryon density are plotted for the three different cases. The resulting points for the different approaches suggest an equation of state which is fairly stiff by the standards of field theoretical models [3,4] which have been used to describe the behavior of nuclear matter at normal density.

Discussion and Conclusions

It is important to note that the two models used to extract the equation of state have quite different assumptions about the mean free paths of the particles in the system. The cascade model has a long mean free path ($\lambda_{mfp} \gtrsim R$) and the chemical model with shock compression a short mean free path ($\lambda_{mfp} \ll R$) assumption relative to the size R of the system. The similarities of the results perhaps reflects the fact that equilibrium is reached in both approaches during the high density stage and that the chemistry that produces the pions is similar in both cases. Furthermore, either the pion production is insensitive to the dynamics of the compression and expansion stages or the dynamics in the two approaches are in fact very similar. Recent results from Ref.[26] shed some light on this subject. Displayed in Fig.9 are shock compression curves (for various assumptions about the equation of state) of the baryon density as a function of incident energy in nucleus-nucleus collisions. Also plotted are cascade points (crosses) for the Ar + Ca system. The ideal gas (curve 1) yields the highest densities, almost a factor of two higher than any other. So the cascade is not an ideal gas. However, when an Enskogg-corrected [30] ideal gas calculation (curve 2) is made the results agree very well with the cascade predictions. Thus, the finite range of the hadronic forces which is incorporated in the cascade via the scattering mechanism and cross sections accounts for this difference and the cascade in fact does reach shock densities. The other curves in Fig.9 correspond to the densities for various equations of state which include compressional energy. Presented in Fig.10 are the predictions for the pion to participant ratio as a function of energy for these same shock compression models and the cascade model. All the equations of state overpredict the pion yield except for the quadratic form with incompressibility constant $K = 800$ MeV. In these calculations the system is also treated as a degenerate Fermi gas with the Fermi degeneracy energy included.

A similar hydrodynamics calculation [31] employing the quadratic form of the equation of state yields a fit to the pion to participant ratio for $K \approx 300$ MeV. The predictions of this model are presented in Fig.11 for several incompressibility constants. It seems necessary for these approaches to use a quadratic form rather than a linear form of the equation of state to be able to fit the data. A linear form will not generate enough compressional energy. In fact, it should be pointed out that the value of the incompressibility constant is determined at $\rho = \rho_0$. The actual parametrizations of the equation of state can vary such that the incompressibility constant alone is meaningless without stating the form. Nevertheless, the two aforementioned calculations [26,31] yield similar qualitative conclusions (the equation of state is very stiff) but different quantitative results (incompressibilities) for identical parameterizations of the equation of state.

Another approach, using the Boltzmann equation [32] with a Skyrme force, comes very close to predicting the pion to participant ratio as a function of energy. This is seen in Fig.12 where the cascade and Boltzmann equation predictions are displayed along with the Ar + KCl data. The predictions are still slightly higher than the observed ratios. This equation of state is somewhat stiffer than the previous hydrodynamic calculation [31], but softer than that of Sano [26]. Both studies found that an increasing amount of compressional energy was necessary to decrease the pion yield.

In summary, both chemical and thermal equilibrium rate calculations and cascade model analyses suggest that chemical freeze-out of the pion-like degree of freedom occurs at the onset of expansion. The pion multiplicity observed in the final state should then reflect the conditions of the high density stage where chemical and thermal equilibrium are expected to occur. A schematic hydrodynamic model consisting of chemical and thermal equilibrium and shock compression was used to describe the high density stage. This model and the intranuclear cascade model were independently compared to the pion production data in order to determine the compressional energy of the system at various incident energies. It is necessary to stress the assumptions made in this approach. The flow kinetic energy, if present in the high density stage, was ignored and all the kinetic energy was considered to be thermalized and available for pion production. Also, any dilute surface effects due to the finite size of the nuclear system, and medium corrections [33] to the specific heat of the N,Δ and π gas were ignored. Corrections for such effects, if present, would tend to lower the extracted compressional energies and soften the equation of state. Furthermore, the role of the Fermi degeneracy energy [26] has been disregarded in extracting the compressional energies in both the cascade and chemical model calculations. The resulting compressional energies should only be considered as a first estimate of the nuclear equation of state at high densities with more refined theoretical calculations necessary to identify the effects of possible corrections and to specify the precise form of the equation of state. In any case it appears that the equation of state is fairly stiff and rises rather linearly above densities of $3\rho_0$ in agreement with recent field theoretical calculations [3,4].

We would like to thank M. Gyulassy and H. Stöcker for interesting and helpful discussions, and for the use of their material prior to publication. We especially wish to thank G.D. Westfall for the thermal model results.

This work was supported in part by the Director, Office of Energy Research, Division of Nuclear Physics of the Office of High Energy and Nuclear Physics of the U.S. Department of Energy under Contract DE-AC03-76SF00098.

REFERENCES

1. H.A. Bethe, G.E. Brown, J. Applegate and J.M. Lattimer, Nucl. Phys. A324 (1979) 487.
2. M. Nauenberg and G. Chapline, Astrophys. Journ. 179 (1973) 277.
3. J. Boguta and H. Stöcker, Phys. Lett. 120B (1983) 289.
4. J.D. Walecka, Proceedings of the 5th High Energy Heavy Ion Study, LBL Report 12652 (1981) 91.
5. J. Cugnon, T. Mitzutani and J. Vandermeulen, Nucl. Phys. A352 (1981) 505;
   J. Cugnon, D. Kinet and J. Vandermeulen, Nucl. Phys. A379 (1982) 553.
6. H.G. Ritter, K.G.R. Doss, H.A. Gustafsson, H.H. Gutbrod, B. Kolb, H. Löhner, B. Ludewigt, A.M. Poskanzer, T. Renner, A. Warwick and H. Wieman, Proceedings of this Conference.
7. H.A. Gustafsson, K.G.R. Doss, H.H. Gutbrod, B. Kolb, H. Löhner, B. Ludewigt, A.M. Poskanzer, T. Renner, H.G. Ritter, A. Warwick and H. Wieman, Proceedings of this Conference.
8. G.F. Chapline, M.H. Johnson, E. Teller and M.S. Weiss, Phys. Rev. D8 (1973) 4302.
9. M.I. Sobel, P.J. Siemens, J.P. Bondorf and H.A. Bethe, Nucl. Phys. A251 (1975) 502.
10. H. Stöcker, W. Greiner and W. Scheid, Z. Phys. A286 (1978) 121.
11. P. Danielewicz, Nucl. Phys. A314 (1979) 465.
12. A. Sandoval, R. Stock, H.E. Stelzer, R.E. Renfordt, J.W. Harris, J.P. Brannigan, J.V. Geaga, L.J. Rosenberg, L.S. Schroeder and K.L. Wolf, Phys. Rev. Lett. 45 (1980) 874.
13. M.Kh. Anikina, K. Beshliu, G.L. Vardenga, M. Gazdzitskii, A.I. Golokhvastov, T.D. Dzhobava, S.N. Komarova, E.S. Kuznetsova, Yu. Lukstyn'sh, E.O. Okonov, T.G. Ostanevich, V. Topor and S.A. Khorozov, Sov. J. Nucl. Phys. 38 (1983) 901.
14. R. Hagedorn and J. Ranft, Suppl. Nuovo Cimento 6 (1968) 169.
15. J.I. Kapusta, Phys. Rev. C16 (1977) 1493.
16. A.Z. Mekjian, Nucl. Phys. A312 (1978) 491.
17. S. das Gupta and A.Z. Mekjian, Phys. Reports 72 (1981) 131.
18. J. Gosset, H.H. Gutbrod, W.G. Meyer, A.M. Poskanzer, A. Sandoval, R. Stock and G.D. Westfall, Phys. Rev. C16 (1977) 629.

19. G. Bertsch and J. Cugnon, Phys. Rev. C24 (1981) 2514.

20. J.W. Harris and R. Stock, LBL Report 17054 (1984) and Proceedings of the 7th Oaxtepec Simposium on Nucl. Phys., Notas de Fisica 7 (1984) 61; J.W. Harris, R. Stock, R. Bock, R. Brockmann, A. Sandoval, H. Ströbele, G. Odyniec, H.G. Pugh, L.S. Schroeder, R.E. Renfordt, D. Schall, D. Bangert, W. Rauch and K.L. Wolf, to be published in Phys. Lett. B.

21. H. Stöcker, J. Phys. G10 (1984) L111.

22. R. Brockmann, J.W. Harris, A. Sandoval, R. Stock, H. Ströbele, G. Odyniec. H.G. Pugh, L.S. Schroeder, R.E. Renfordt, D. Schall, D. Bangert, W. Rauch and K.L. Wolf, Phys. Rev. Lett. 53 (1984) 2012.

23. D. Beavis, S.Y. Fung, W. Gorn, A. Huie, D. Keane, J.J. Lu, R.T. Poe, B.C. Shen and G. Van Dalen, Phys. Rev. C27 (1983) 910.

24. P. Siemens and J.I. Kapusta, Phys. Rev. Lett. 43 (1979) 1486.

25. J.I. Kapusta and D. Strottmann, Phys. Rev. C23 (1981) 1282.

26. M. Sano, M. Gyulassy, M. Wakai and Y. Kitazoe, submitted to Phys. Lett. B.

27. R. Stock, R. Bock, R. Brockmann, J.W. Harris, A. Sandoval, H. Stroebele, K.L. Wolf, H.G. Pugh, L.S. Schroeder, M. Maier, R.E. Renfordt, A. Dacal and M.E. Ortiz, Phys. Rev. Lett. 49 (1982) 1236.

28. J. Gosset,J.I. Kapusta and G.D. Westfall, Phys. Rev. C18 (1978) 844 and G.D. Westfall private communication.

29. A.Z. Mekjian, Phys. Rev. C17 (1978) 1051.

30. R. Malfliet, Nucl. Phys. A420 (1984) 621.

31. J. Molitoris and H. Stöcker, MSU Preprint MSUCL-498 (1984) and in Proceedings of this Conference.

32. H. Kruse, B. Jacak and H. Stöcker, MSU Preprint MSUCL-470 (1984) to be published in Phys. Rev. Lett. and H. Stöcker in Proceedings of this Conference.

33. I.N. Mishustin, F. Myhrer and P.J. Siemens, Phys. Lett. 95B (1980) 361.

34. Y. Yariv and Z. Fraenkel, Phys. Rev C20 (1979) 2227 and C24 (1981) 488. Y. Yariv, private communication.

Figure Captions

1. Predictions of the intranuclear cascade model [5] for central collisions ($b \leq$ 3.4 fm.) of 1.0 GeV/n $^{139}La + {}^{139}La$. The time dependence in units of fm/c is presented on a semi-logarithmic scale for the (a) baryon density in units of normal nuclear density ρ_0, (b) number of baryon-baryon collisions per unit time and (c) the instantaneous number of pions + delta resonances (scale on right). Also displayed as a bar in (c) is the prediction of a simple

chemical model for the equilibrium abundance at the predicted maximum cascade density.

2. Mean pion multiplicity $< n_\pi >$ per nucleon as a function of incident energy predicted by the hydrodynamic model of Ref.[10]. (a) Results of a soft ($K_0 = 100$ MeV) and a stiff ($K_0 = 300$ MeV) nuclear equation of state are shown. (b) Results of a calculation with a density isomer in the equation of state. Curve a is the normal nuclear matter curve ($K_0 = 300$ MeV) and curves b and c have secondary minima in the equation of state at $\rho = 5\rho_0$ with binding energies $B_1 = 0$ and -140 MeV, respectively, as depicted in the insert.

3. The energy dependence of the mean negative pion multiplicity $< n_{\pi^-} >$ for central collisions of Ar + KCl from Ref. [12]. Above 100 MeV c.m. energy the data can be fitted by a straight line.

4. Maximum density as a function of incident energy predicted by the cascade model for Ar + KCl. The circles represent the mean density weighted by the $\pi + \Delta$ production rate.

5. The mean negative pion multiplicity observed in Ar + KCl reactions at 1.0, 1.2, 1.4, 1.6 and 1.8 GeV/n as a function of the observed number of proton participants Q from Ref. [20]. Only the interpolating lines are shown except for 1.0 and 1.8 GeV/n.

6. The multiplicity of pions plus deltas per participant plotted as a function of c.m. energy (lower axis) and laboratory energy (upper axis) for Ar + KCl. The solid curves are the experimental points for zero impact parameter. The dashed and dotted curves are the Cugnon cascade and the chemical model results for the $< n_\pi + n_\Delta >$ per participant dependence on the thermal energy (E_T) and the triangles are the predictions of the Yariv-Fraenkel [34] cascade. The horizontal arrows represent the values of the compressional energy per nucleon E_c determined at each experimental point as described in the text.

7. The mean π^- multiplicity as a function of incident energy for central collisions of Ar + KCl (open triangles) with $b \lesssim 0.33 b_{max}$ and La + La (solid triangles-preliminary) with $b \lesssim 0.25 b_{max}$ assuming a geometrical model for the trigger cross section. The corresponding cascade model calculations are drawn as open and solid circles, respectively. The horizontal arrows represent the compressional energy deduced from a comparison with the cascade model.

8. Values of the ground state nuclear matter energy $W(\rho, T = 0)$ presented as a function of the density in units of normal nuclear matter density ρ_0. The points are derived from the Ar + KCl minimum bias data extrapolated to zero impact parameter using the cascade (triangles) and chemical models (circles) independently. Also shown are preliminary points from the La + La central trigger data using the cascade (boxes). Only statistical errors are given.

9. The baryon density as a function of the c.m. kinetic energy per nucleon

assuming shock compression (curves 1-5) from Ref.[26] and for the cascade (crosses). Curve 1 is the result for an ideal gas. Curve 2 is an ideal gas with Enskogg correction. Curves 3 and 4 include a quadratic form of the potential with $K = 250$ and 800 MeV, respectively, and curve 5 corresponds to a linear form with $K = 800$ MeV.

10. The pion to participant ratio as a function of c.m. energy. The curves are labeled as in Fig.9. The solid circles are the data points extrapolated to zero impact parameter for Ar + KCl. Curve S corresponds to an interpretation [26] of the empirical equation of state derived from the chemical model analysis.

11. The pion to participant ratio predicted by a hydrodynamic model [31] as a function of energy for several incompressibility constants assuming a quadratic form of the equation of state.

12. Predictions for the negative pion multiplicity using a Boltzmann equation approach [32] and a cascade model. Also shown are the data[12].

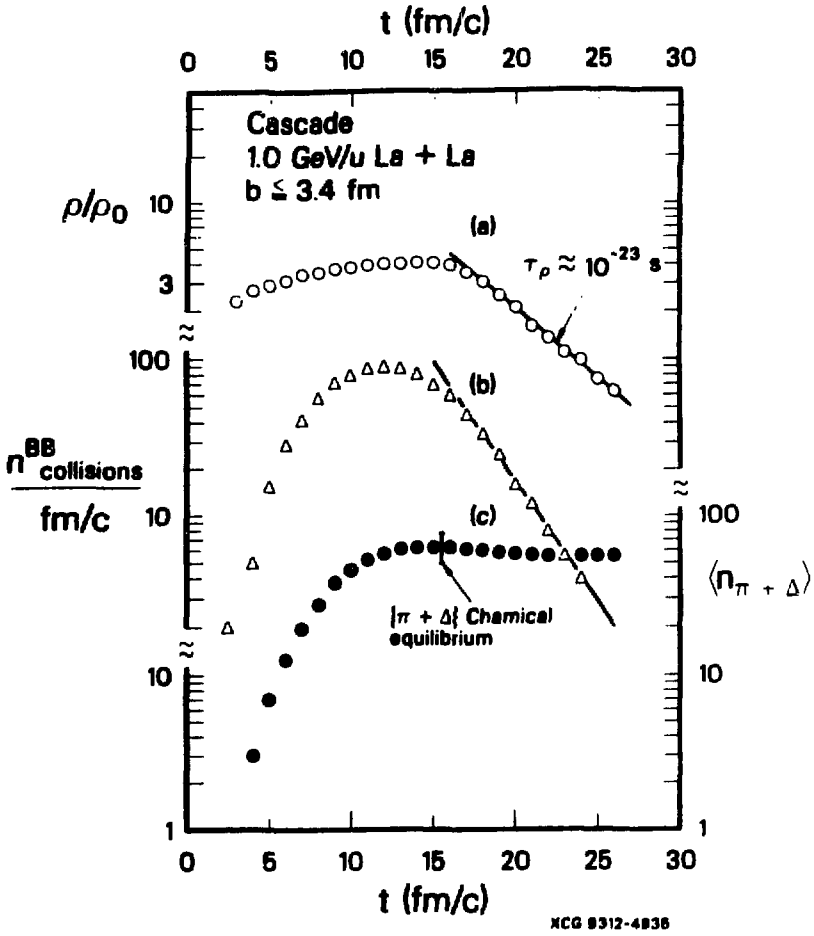

Figure 1

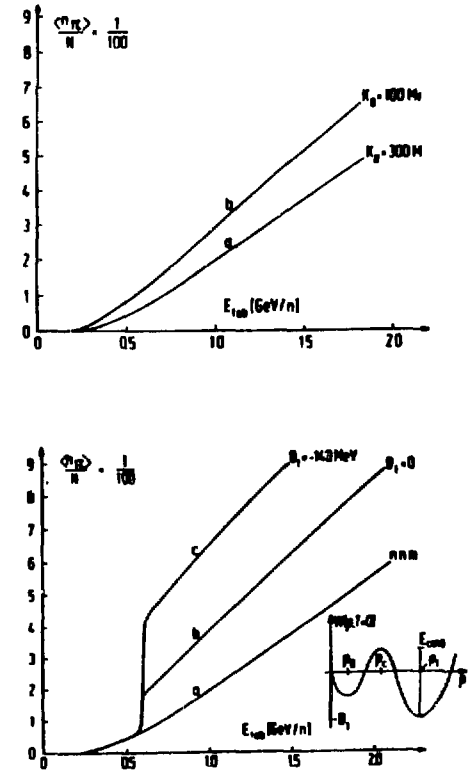

Figure 2

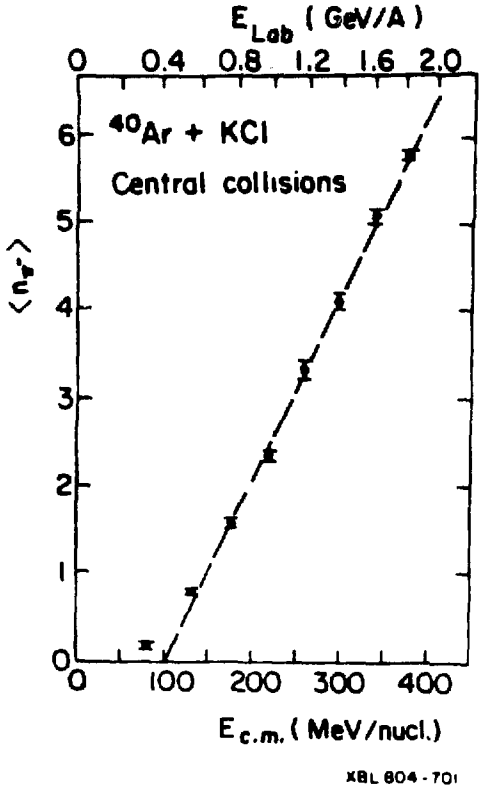

Figure 3

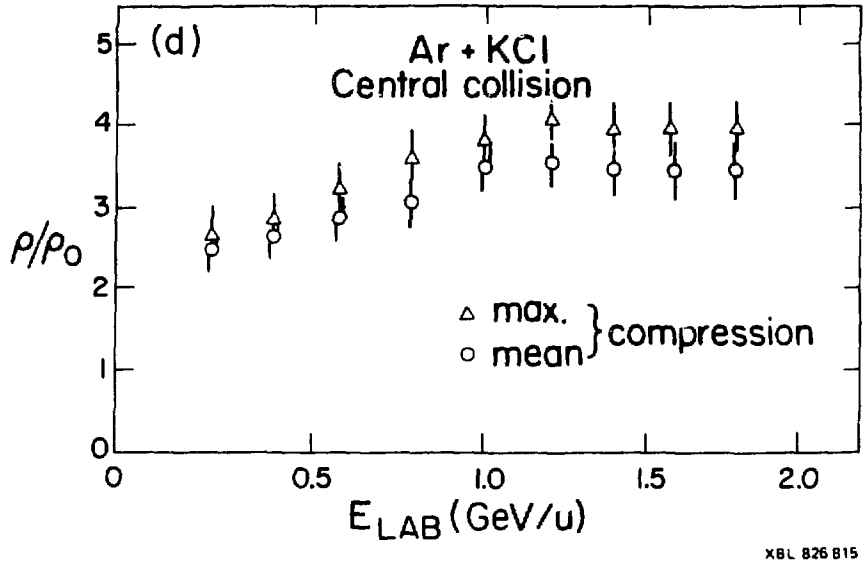

Figure 4

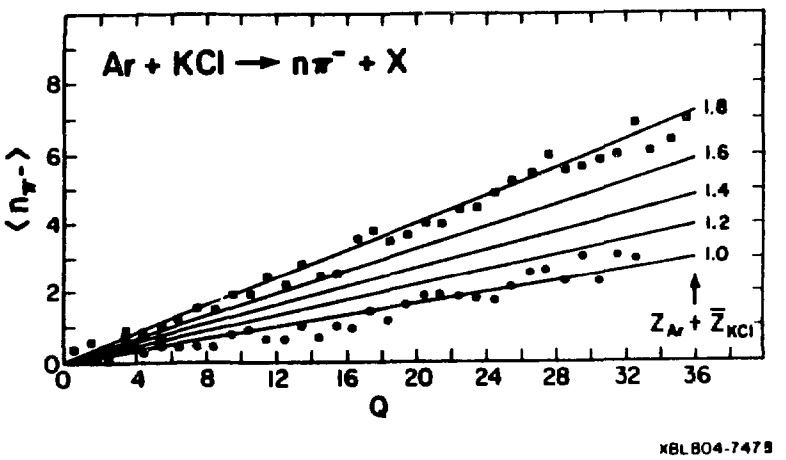

Figure 5

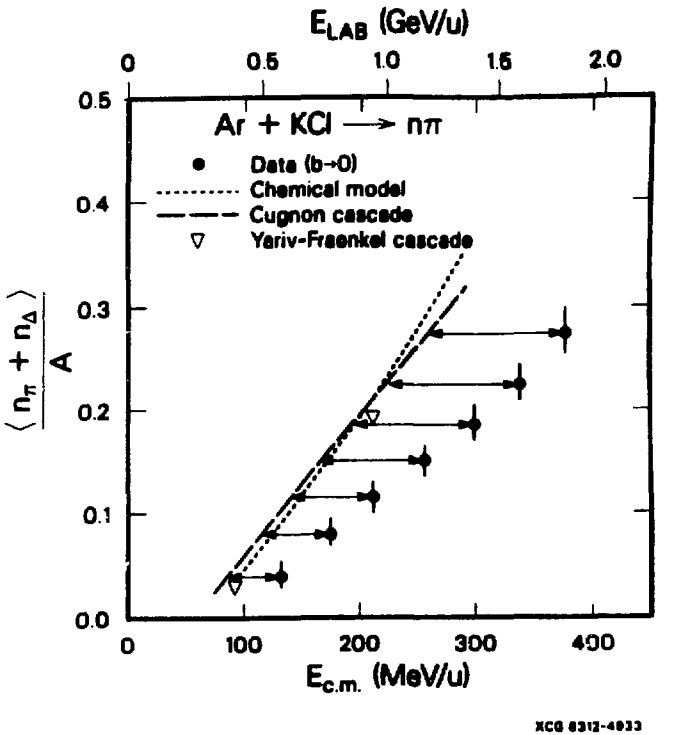

Figure 6

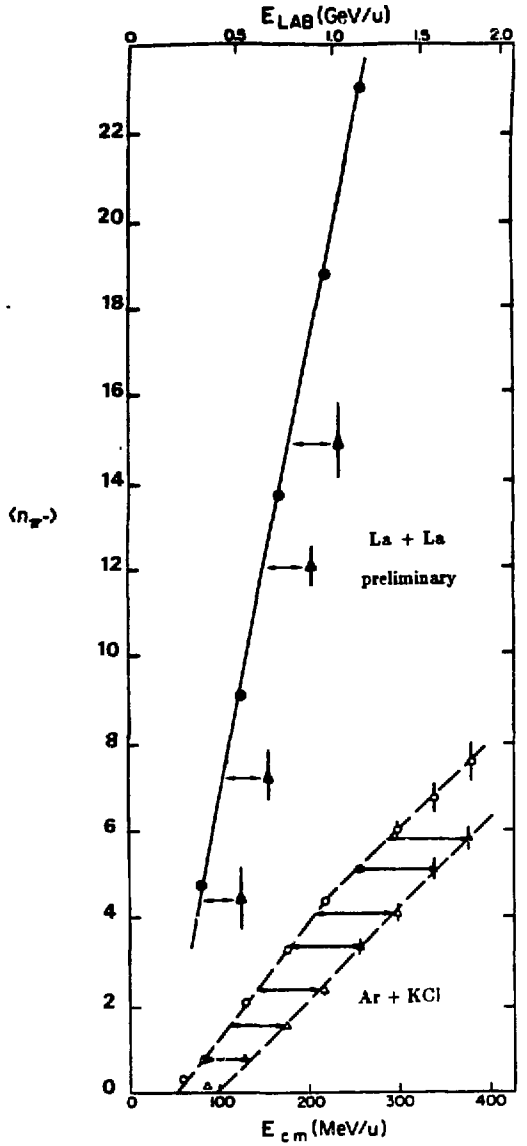

Figure 7

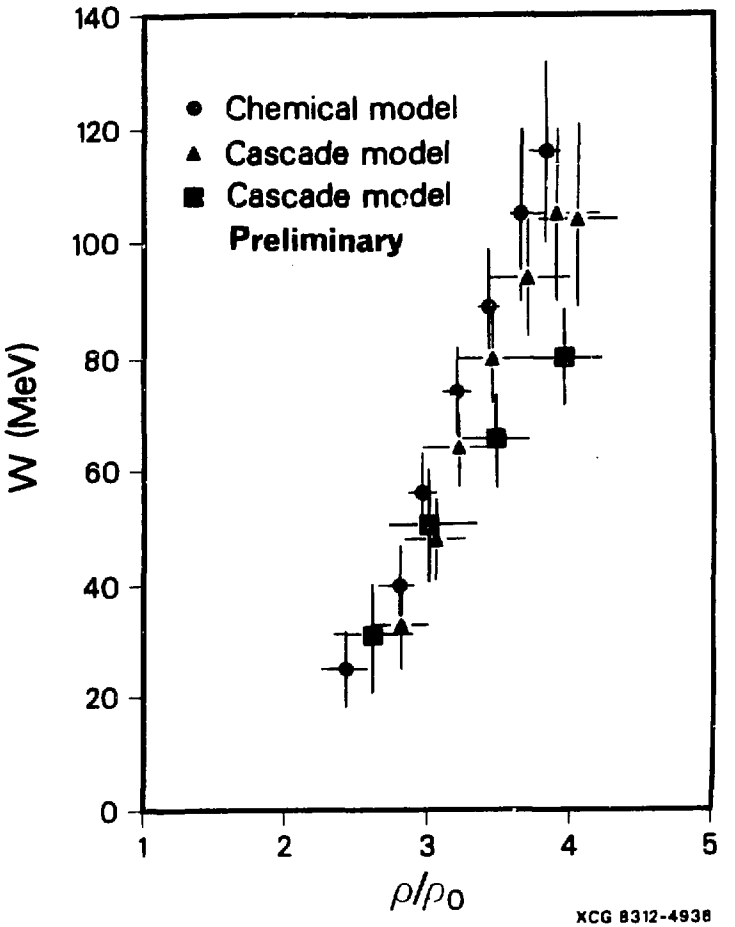

Figure 8

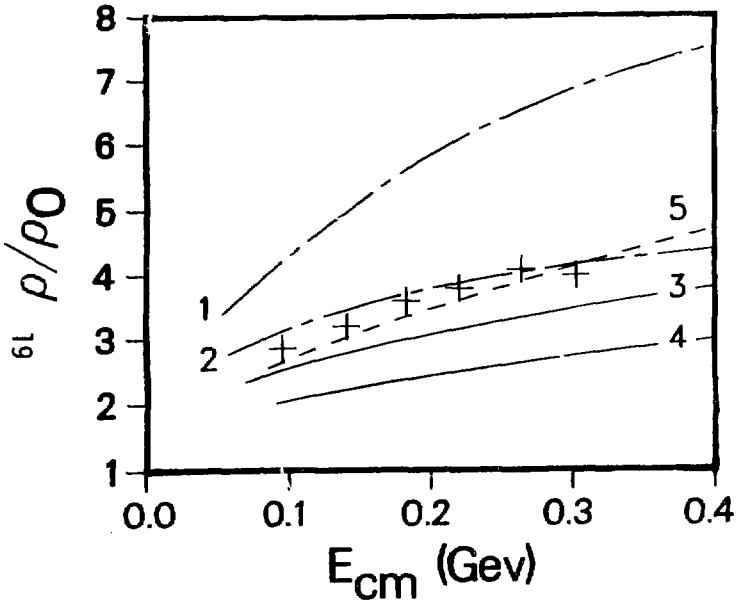

Figure 9

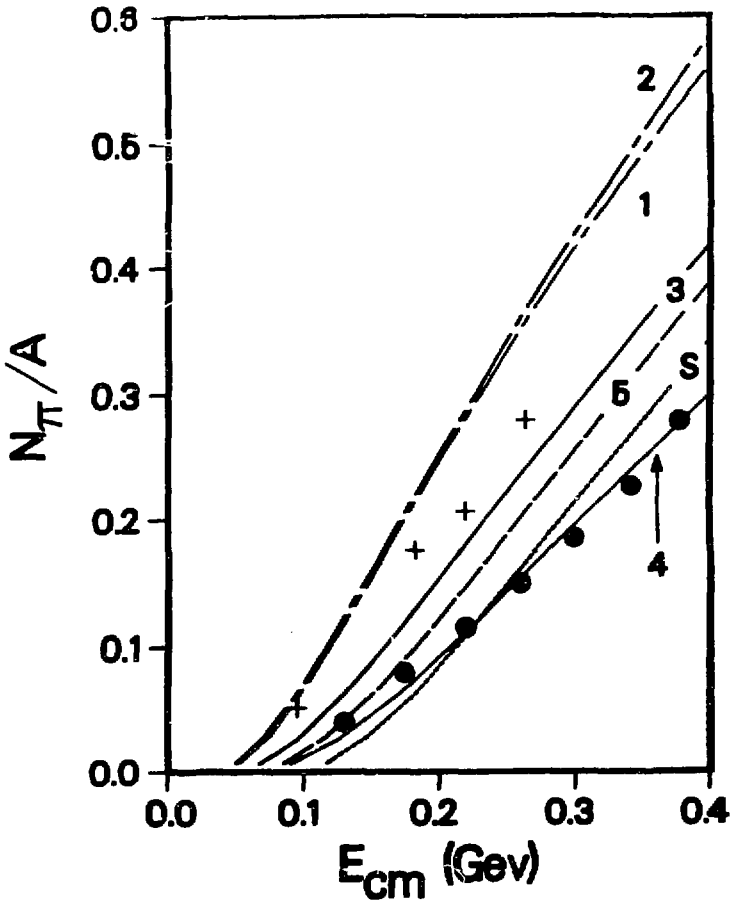

Figure 10

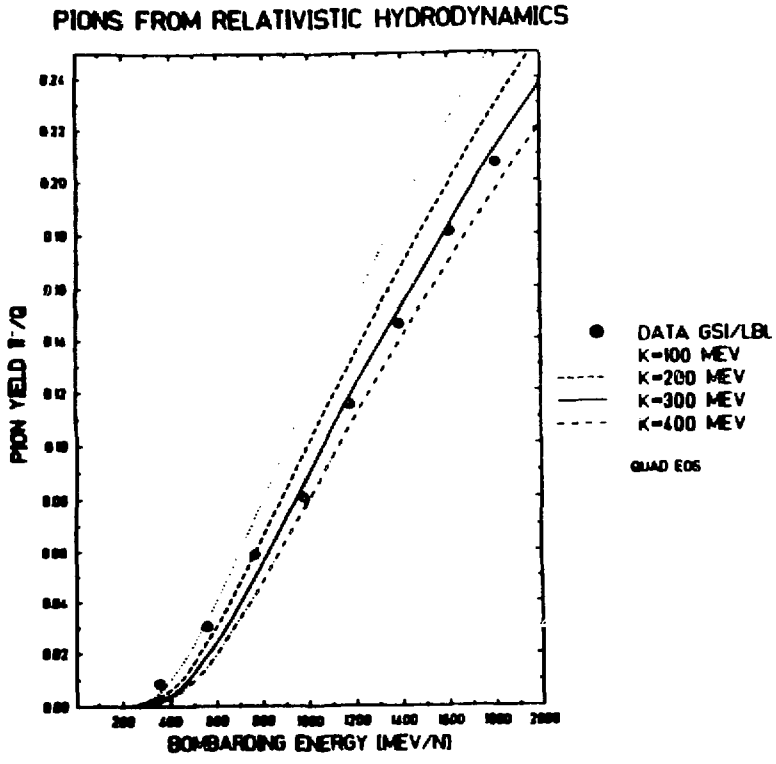

Figure 11

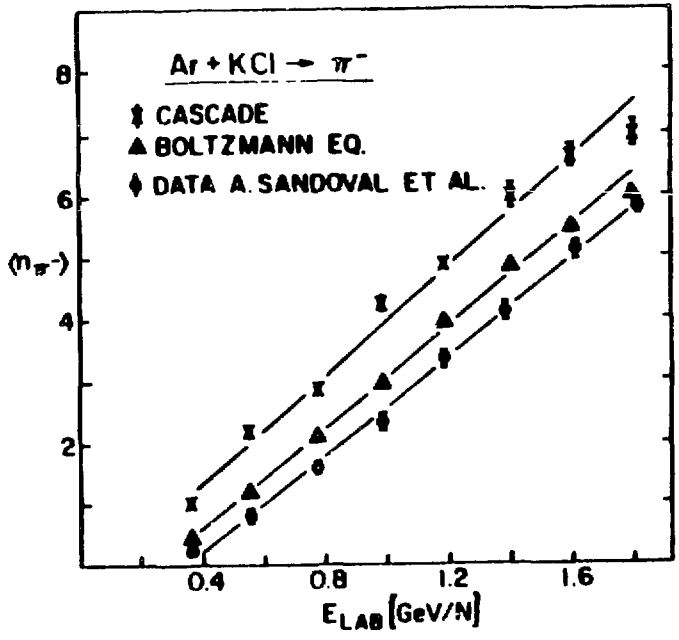

Figure 12